HHS Public Access

Author manuscript

J Control Release. Author manuscript; available in PMC 2021 October 04.

Published in final edited form as:

J Control Release. 2021 September 10; 337: 144–154. doi:10.1016/j.jconrel.2021.07.012.

Pilot-scale production of expansile nanoparticles: Practical methods for clinical scale-up

Aaron H. Colby[a,b,*], **Rong Liu**[c], **Robert P. Doyle**[d], **Alyssa Merting**[e], **Heng Zhang**[f], **Natasha Savage**[e], **Ngoc-Quynh Chu**[c], **Beth A. Hollister**[g], **William McCulloch**[h], **Joanna E. Burdette**[i], **Cedric J. Pearce**[j], **Kebin Liu**[e], **Nicholas H. Oberlies**[k], **Yolonda L. Colson**[c], **Mark W. Grinstaff**[a,b,f]

[a]Boston University, Department of Biomedical Engineering, Boston, MA, United States of America

[b]Ionic Pharmaceuticals, LLC, Brookline, MA, United States of America

[c]Massachusetts General Hospital, Boston, MA, United States of America

[d]PCI Synthesis, Newburyport, MA, United States of America

[e]Augusta University, Augusta, GA, United States of America

[f]Boston University, Department of Chemistry, Boston, MA, United States of America

[g]HighRock Consulting, Oxford, NC, United States of America

[h]Alba BioPharm Advisors, Inc., Raleigh, NC, United States of America

[i]University of Illinois at Chicago, College of Pharmacy, Chicago, IL, United States of America

[j]Mycosynthetix, Inc., Hillsborough, NC, United States of America

[k]University of North Carolina at Greensboro, Department of Chemistry and Biochemistry, Greensboro, NC, United States of America

Abstract

One of the foremost challenges in translating nanoparticle technologies to the clinic is the requirement to produce materials on a large-scale. Scaling nanoparticle production methods is often non-trivial, and the success of these endeavors is frequently governed by whether or not an intermediate level of production, i.e., “pilot-scale” production, can be achieved. Pilot-scale production at the one-liter scale serves as a proof-of-concept that large-scale production will be possible. Here, we describe the pilot-scale production of the expansile nanoparticle (eNP) technology including verification of activity and efficacy following scaleup. We describe the challenges of sonication-based emulsification procedures and how these were overcome by use of a Microfluidizer technology. We also describe the problem-solving process that led to pre-polymerization of the nanoparticle polymer—a fundamental change from the lab-scale and

*Corresponding author at: Boston University, Department of Biomedical Engineering, Boston, MA, United States of America. acolby@bu.edu (A.H. Colby).

Appendix A. Supplementary data

Supplementary data to this article can be found online at https://doi.org/10.1016/j.jconrel.2021.07.012.

previously published methods. Furthermore, we demonstrate good control over particle diameter, polydispersity and drug loading and the ability to sterilize the particles via filtration using this method. To facilitate long-term storage of these larger quantities of particles, we investigated six lyoprotectants and determined that sucrose is the most compatible with the current system. Lastly, we demonstrate that these changes to the manufacturing method do not adversely affect the swelling functionality of the particles, their highly specific localization to tumors, their non-toxicity in vivo or their efficacy in treating established intraperitoneal mesothelioma xenografts.

Keywords

Pilot-scale production; Expansile nanoparticle; Microfluidizer; Scale-up; Clinical translation

1. Introduction

One of the foremost challenges in translating nanoparticle technologies to the clinic is the need to produce materials at large scales, to say nothing of the requirements of current Good Manufacturing Practice (cGMP) production [1–3]. Numerous publications describe the small, laboratory-scale synthesis and testing of nanoparticles [4–7]. While far fewer in number, there are also several “success stories” of nanoparticles that have been successfully scaled-up and translated to the clinic (e.g., Abraxane, Doxil, CRLX101). Yet, between the early-stage “lab-scale” and clinical-stage “large-scale” production of nanoparticles lies a critical and rarely discussed or published realm, that of “pilot-scale” production. For this discussion, lab-scale refers to quantities on the order of <100 mL or grams, pilot-scale to 100–1000 mL or grams, and large-scale as multi-liter or kilogram.

Pilot-scale production is the first unheralded step in the development of large-scale production en route to clinical evaluation and commercialization. As such, it is often the first process tackled by companies seeking to commercialize a technology that has proven successful at the lab-scale. However, despite the importance of this development step to the commercialization of the technology, it can be perceived as less novel or exciting in comparison to new and cutting-edge proof-of-concept studies. However, innovation is central to this step in the translation process. Reasons for the lack of publications regarding pilot-scale production may include: that results of failed projects are rarely published; there is general lack of public funding to pursue these types of studies; and, when projects do succeed, investigators and companies may be incentivized to keep their methods as “trade secrets” to keep ahead of competition in the marketplace. Lastly, from an academic perspective, it may be easier and more rewarding to pivot to another nanoparticle formulation—for example by changing the drug-loading, targeting ligand, size, surfactant etc.—than to tackle the challenges of scale-up and translation.

Herein, we describe our efforts to commercialize a polymeric nanoparticle drug delivery technology for the treatment of peritoneal tumors and, specifically, the development of pilot-scale production methods. These pH-responsive nanoparticles, which swell and expand in response to a mildly acidic pH, are termed “expansile nanoparticles” or “eNPs” (Fig. 1). eNPs use a unique Materials-Based Targeting strategy to achieve tumor specific

localization to intraperitoneal tumors when administered intraperitoneally [8–10]. Previous studies demonstrate the ability of eNPs to: provide pH-triggered swelling and drug release [11–14]; localize to tumors with >92% specificity [8]; yield 10–100-fold higher tumoral drug concentrations than the "free" drug or clinical formulation controls [10]; and, more than double animal survival compared to these clinically used free-drug controls [10]. These, and other, studies are summarized in a comprehensive review by Colby et al [9]. With these data in hand, NIH SBIR funding was secured to address key go/no-go, proof-of-concept studies on the critical path to translation and commercialization of the eNP technology. Specifically, we report the scale-up to pilot-scale production as well as the trouble-shooting process required, which included: a re-design of the nanoparticle formation method, pilot-scale synthesis of the eNP monomer, monomer polymerization, transfer of the emulsification process from sonication-based method to a microfluidics-based method with subsequent optimization, shelf-life stability and sterilization and, finally, confirmation that these changes, needed to achieve pilot-scale production, did not diminish the performance or in vivo efficacy of the system (Fig. 2).

2. Results and discussion

2.1. Pilot-scale synthesis of eNP monomer

We began the scale-up process with the eNP monomer. The two-step synthesis of this material was previously performed on a 1–2 g scale. The reaction was first scaled up to a 50 g scale, then to a 100 g and, finally, 1 kg scale. No difficulties were encountered with the synthesis at the 1 kg scale and good yields were obtained (98% 1st step; 85% 2nd step; 83% overall; Fig. 3A). Of note, the final product was recrystallized from dichloromethane —a purification technique not previously found to succeed at the smaller 1–2 g lab-scale. Importantly, recrystallization of the final product is amenable to pilot-scale production and, in contrast to the previous silica gel column chromatography purification technique, requires less solvent, fewer hours of labor, is less expensive and leads to a pure product. Representative photographs of stages of the synthesis (Fig. 3B) demonstrate one of the less obvious challenges to scale-up, which is the sheer size, volume and weight of glassware and reagents, a factor not present in lab-scale synthesis. The final product was characterized by ^{1}H nuclear magnetic resonance (^{1}H NMR; Supplementary Fig. 1A) and elemental analysis (61.86% carbon, 7.22% hydrogen, 29.82% oxygen; theoretical values: 62.28%, 7.15%, 30.56%, respectively) and a purity of >99.9% determined via high-performance liquid chromatography (HPLC; Supplementary Fig. 1B).

2.2. Re-designing the eNP manufacturing process

With pilot-production of the eNP monomer accomplished, we began scaling the mini-emulsion and base-catalyzed polymerization procedure used to synthesize the eNPs [11]. This process was initially scaled up from a volume of 2 mL per batch to 10 mL per batch. The emulsion and polymerization procedures performed as expected and produced 30–50 nm diameter particles with a high encapsulation efficiency of paclitaxel (80–100%). However, the polydispersity (PDI) of these particles was found to be unacceptably high (average PDI = 0.19)—a PDI of ≤0.1 is nominally considered a "narrow" distribution. We hypothesize that this polydispersity results from the significant variability in shear stress

experienced by the dichloromethane droplets as a function of distance from the tip of the sonicator probe. We evaluated the impact of stirring the solution during sonication as well as increasing the relative amount of sodium dodecyl sulfate surfactant from 24% wt/wt (e.g., 24 mg surfactant/100 mg eNP-monomer) to 48% wt/wt. However, neither of these strategies resulted in significant improvements (i.e., lowered) PDI.

As an alternative to probe-sonication and mini-emulsion polymerization, we evaluated the utility of an LV1 Microfluidizer high-shear device (Microfluidics Corp.) for producing nanoparticles with more well-controlled particle diameters and PDIs. The concept behind the Microfluidizer technology is shown schematically in Fig. 4. Specifically, a pre-emulsified, polydisperse suspension is hydraulically driven through a small Y-shaped interaction chamber. The two streams from the Y-junction are forced together at an intersection, causing the droplets to collide in a high-energy impact zone. The shear stresses resulting from these high-energy collisions result in reduced droplet size. Because all droplets are processed through the same micro-channel, similar shear stresses are experienced by the entire sample leading to more homogeneous size distributions and a lower PDI than are achieved with probe-tip systems.

Interestingly, we discovered that the LV1 produced stable emulsions but the in situ, base-catalyzed polymerization of the eNP monomer failed to initiate. One possible explanation is that the heat generated during the LV1 processing caused degradation of the initiator. Significant heating of the sample can occur as a consequence of the high-pressure shearing (15,000 PSI; 100 MPa) of the LV1 process. Heat is generated in the suspension at approximately ~1 °C/processing pass for every 1000 PSI (7 MPa) of processing pressure with potentially higher instantaneous temperatures. An ice bath was used to cool the solution during processing; however, polymerization was still ineffective.

To circumvent this problem of failed in situ polymerization, we performed a series of pilot experiments to determine if processing a pre-polymerized hydrophobic polymer under the same emulsification conditions formed nanoparticles. For the initial tests, we employed the generic polymer poly(lactic-*co*-glycolic) acid (PLGA; MW 30 kDa). Nanoparticles of approximately 100 nm diameter with (PDI <0.1) were readily obtained by dissolving PLGA in dichloromethane (0.83 mM) and emulsifying in a pH 7.4 phosphate buffer containing sodium dodecyl sulfate followed by stirring the ensuing suspension under open air to allow evaporation of the solvent.

Having demonstrated the feasibility of the LV1-based approach with PLGA, we investigated this alternative manufacturing strategy for the eNPs by pre-polymerizing the monomer prior to emulsion thereby alleviating the need for the emulsion-based in situ polymerization. Fig. 5 summarizes these two strategies and highlights the differences between the original route and this new route. To polymerize the eNP monomer, we employed a free-radical polymerization using azobisisobutyronitrile (AIBN) as the initiator (Fig. 6A). This polymerization scheme was chosen because it is facile, robust and readily transferrable to larger-scale production. The molecular weight (MW) of the polymer (characterized by gel permeation chromatography, GPC) was tuned by varying the amount of initiator from 10%

wt/wt AIBN/eNP monomer (MW ~11 kDa) to 0.25% wt/wt AIBN/eNP monomer (MW ~39 kDa; Fig. 6B).

Two factors were determinative in selecting the molecular weight of the eNP polymer. First, polymers with a MW greater than ~30 kDa were frequently found to be insoluble in dichloromethane at a concentration of 25 mg/mL—the concentration required for the nanoparticle synthesis procedure—and, therefore, the target MW needed to be lower. Second, the PDI of the polymer was significantly higher for the lower MW polymers (<15 kDa) while not being significantly different between 18 kDa and 30 kDa. Therefore, 20–25 kDa was selected as the target MW for future studies.

2.3. Pilot-scale synthesis of eNP polymer

The addition of the polymerization step prior to nanoparticle formation necessitated the scale-up of this synthetic procedure. As with the monomer scale-up, the reaction was first performed on a 1–10 g scale, followed by a 50 g and 100 g scale prior to a 1 kg scale. No significant challenges were encountered with regard to chemical reactivity, polymer size or purification as the reaction scale increased. As with the monomer synthesis, the sheer size and volume of reagents required (e.g., 60+ liters of methanol for washing) are a logistical and physical challenge (Fig. 6C). Nevertheless, we synthesized the eNP polymer on the kilogram-scale with structure confirmed by ^{1}H NMR, ^{13}C NMR, IR and MW by GPC (SI Fig. 2).

2.4. Pilot-scale synthesis of PTX-eNPs via Microfluidizer homogenization

Next, paclitaxel-loaded eNPs (PTX-eNPs) were produced using the LV1 and eNP polymer. The LV1 is capable of producing processing pressures of 5000 PSI (30 MPa) to 30,000 PSI (200 MPa). However, the heat generated at 30,000 PSI was incompatible with the volatile dichloromethane solvent, even when using a pre-cooled solution and ice bath around the LV1's plumbing. Particle suspensions generated at 5000 PSI were larger (>1 μm) than the target specification of 30–50 nm. We therefore selected 15,000 PSI (100 MPa) as the processing pressure to evaluate the impact of the number of processing passes. The results of processing either 1, 2, 3, 5, 7 or 10 times through the LV1 using either 24% wt/wt (e.g., 24 mg surfactant/100 mg eNP-polymer), 48% wt/wt or 96% wt/wt surfactant are presented in Fig. 7. Average particle diameter tended to decrease during the first three processing passes, regardless of the amount of surfactant, and plateaued thereafter. Increasing the surfactant ratio from the previously "standard" 24% wt/wt to 48% wt/wt and finally 96% wt/wt resulted in corresponding decreases in particle diameter after three processing passes from 44 nm to 37 nm and 23 nm, respectively. While increasing the relative amount of surfactant decreased average diameter even without LV1 processing (i.e., see number of processing passes = 0 in Fig. 7A), the PDI of these distributions remained high (0.1–0.2, Fig. 7B) and the variability in average diameter from one batch to another was large (standard deviation of 20–30 nm). Therefore, a combination of 48% wt/wt surfactant with three processing passes were selected as the optimum parameters moving forward.

Following processing on the LV1, the dichloromethane solvent is evaporated under air—the United States Pharmacopeia (USP) limit for residual solvents was used to set the upper limit

of acceptable residual dichloromethane. Four hours of evaporation leads to residual levels that meet this limit (<600 ppm). The particles were then dialyzed to remove excess salts and surfactant. Dialysis tubing of four different molecular weight cut offs (MWCO) was investigated: 10 kDa, 50 kDa, 300 kDa and 1000 kDa. The 10 kDa MWCO tubing was used historically and this proved to be the most effective. Higher MWCO tubing suffered from varying degrees of particle agglomeration leading to increased average diameters and PDIs (Fig. S3 A–B). Interestingly, the 300 kDa and 1000 kDa MWCO tubing experienced a 40–50% reduction in volume during dialysis which caused the particles to concentrate into a viscous liquid (Fig. S3 C). This may have been due to a sufficiently high rate of water exchange across these membranes that the surfactant was, effectively, actively washed off leading to agglomeration and precipitation of the particles and, subsequently, an osmotic gradient out of the dialysis bag and into the now surfactant-filled sink. We hypothesize that the MWCO-dependent nature of this result may occur because, as SDS is removed from the particles, it forms micelles locally within the dialysis bag—the critical micelle concentration (CMC) for SDS is 0.2% and SDS is present at 1.2% initially—and these micelles are able to diffuse more rapidly through the larger pores of the higher MWCO tubing. Slower rates of diffusion through the lower MWCO tubing would lead to higher retention of SDS and, subsequently, less agglomeration.

Following dialysis, the effect of LV1 processing is readily visible by eye. Particle suspensions were cloudy and opaque when emulsified only via sonication and without the use of the LV1. This cloudiness is likely a reflection of the presence of larger (>400 nm) particles that absorb and refract visible light (Fig. 7C). In contrast, particles that are processed two to three times or more on the LV1 are translucent—a reflection of the more homogeneously small (<50 nm) particle distributions.

As a proof-of-concept demonstration of the control and scalability of the PTX-eNP synthesis, we manufactured a one-liter batch of particles. This pilot-scale batch (Fig. 8) was manufactured within the developed design specifications with a mean diameter of 40 nm, a PDI of 0.1 and a paclitaxel loading of 93%. It is important to note that further scale-up of the manufacturing process would involve moving from a batched processing system (i.e., the LV1) to a continuous flow processing system that is designed to process and produce particles on the multi-liter scale. Such technologies are commercially available, but these are truly “large-scale” systems and are beyond the scope and scale of the current study.

2.5. Sterilization via filtration

Importantly, the small diameter and low PDI of the LV1-produced particles has a practical consquence: these particles can be sterilized via filtration through a 0.22 um syringe. Filtration does not significantly alter diameter, PDI or paclitaxel loading (Fig. S4), which is congruent with the small, <50 nm, average diameter of the particles. This is in contrast to the originally employed sonication-based procedure (Fig. 5A) which yielded particles with an average diameter <100 nm but a PDI so high that filtration was impossible due to clogging of the filter by the small sub-population of larger (>0.22 um) particles. Filtration is a relatively easy, low-cost method of sterilization and, therefore, this has important implications for the future clinical translation of the technology.

2.6. Lyophilization for long-term stability and shelf-life

The production of nanoparticles on the pilot-scale is only useful inasmuch as these larger volumes can be stored for future use. Historically, PTX-eNPs have demonstrated stability in solution (i.e., no increase in mean diameter or PDI) for at least 24 h with flocculation and precipitation occurring at various times thereafter. To avoid this problem, and to provide storage conditions and durations that would be amenable to the logistical requirements of clinical use, we investigated lyophilization as a means of storage. As has been reported widely [15–17], lyophilization of the particles without use of a lyoprotectant was ineffective. The resuspended particles agglomerated and could not be separated or re-suspended, even via sonication. We therefore screened a series of six commonly used Lyoprotectants at concentrations from 1%–10% wt/vol (Fig. 9A). Lyoprotectants were introduced into the suspension immediately prior to filtration and, following filtration, the particles were frozen and lyophilized. The change in particle diameter from pre-lyophilization to post-resuspension (termed "S_f/S_0") was minimized (i.e., closest to 1.0) using 5% glucose, 5% or 10% sucrose, or 10% trehalose with all other conditions yielding somewhat greater increases in post-resuspension diameter (Fig. 9B). Glucose was not selected because of the unusual behavior wherein the 5% formulation was stable but the 1%, 2% and 10% formulations resulted in significant particle agglomeration. We therefore selected 5% sucrose as the optimal condition, as it required a lesser quantity of lyoprotectant compared to 10% trehalose. Using the 5% sucrose formulation, particles were manufactured and stored in mechanically crimped and stoppered sterile vials. Particles were stored under two environmental conditions: 25 °C + 60% relative humidity (i.e., long term stability testing conditions); and, 40 °C + 75% relative humidity (i.e., accelerated stability testing conditions). Particle diameter was not-significantly different after 1 or 3 months of storage at either condition—these studies are still ongoing (Fig. 9C). These data suggest that lyophilization in the presence of the lyoprotectant sucrose provides a viable means for clinical manufacture and testing.

2.7. Confirmation of pilot-scale formulation performance and in vivo efficacy

To confirm the functionality of the eNP following the change in manufacturing method, the incorporation of a lyoprotectant and the lyophilization and resuspension procedure, we evaluated four performance metrics: 1) particle swelling; 2) in vivo tumor localization; 3) in vivo toxicity; and, 4) in vivo efficacy. Particle swelling is the essential mechanism behind eNP functionality [9,11,12] and can be monitored via scanning electron microscopy (SEM). This robust technique has been used previously to evaluate particle swelling in response to exposure to an acidic environment. Prior studies demonstrate a 2- to 10-fold increase in particle diameter when eNPs are incubated at pH 5 for 24 h with no significant change in diameter when incubated at pH 7.4 [11–13,18]. This same characteristic behavior was observed with particles manufactured on the pilot-scale in this study (Fig. 10A).

Previously, to characterize eNP tumor localization in vivo, we conjugated a rhodamine-methacrylate fluorophore to the eNP backbone thereby allowing visualization by eye under a UV-light source. We used this same strategy to incorporate rhodamine into the eNP polymer and administered paclitaxel-loaded rhodamine-labeled eNPs (PTX-Rho-eNPs) to animals bearing established intraperitoneal tumors according to our previously published

model and protocols [10,18,19]. The PTX-Rho-eNPs performed as expected with significant accumulation in tumors of various sizes, especially in small tumors, throughout the peritoneum (Fig. 10B and Fig. S5).

Multiple studies have demonstrated gross lack of toxicity from treatment with eNPs or PTX-eNPs [8,9,11,12,14,18–21]. To confirm safety of the new, pilot-scale formulation, we treated healthy, non-tumor bearing animals with PTX-eNPs (10 mg PTX/kg body weight) or saline as a control. Over a two-week period post treatment, no adverse clinical observations were made and body weights did not differ significantly between the two groups (Fig. 10C). At 14 days, complete blood counts were taken with no significant differences between PTX-eNP and saline groups (SI Fig. 6A). Because organs of the reticuloendothelial system (e.g., liver and kidney) are the most likely locations for particles to accumulate and, therefore, for toxicity to manifest, we performed liver enzyme profiling prior to sacrifice. Statistical differences in albumin and alanine aminotransferase (ALT) activity were observed between PTX-eNP and saline groups but these were not clinically relevant (SI Table 6B). No differences were observed in total protein, alkaline phosphatase, aspartate aminotransferase (AST), cholesterol, bilirubin or gamma-glutamyl transferase indicating that PTX-eNP do not adversely impact liver function. Furthermore, histopathological evaluation of liver and kidney following sacrifice demonstrated no toxicity in the PTX-eNP group and no differences compared to the saline control (Fig. 10D). Together, these results demonstrate that the modifications to the PTX-eNP manufacturing procedure do not result in unexpected toxicity.

Lastly, to confirm the efficacy of PTX-eNPs produced on the pilot-scale, we employed our previously published model of established intraperitoneal mesothelioma [9,10,18,19]. Animals bearing established intraperitoneal mesothelioma tumors were treated with saline (tumor growth control), paclitaxel dissolved in 50/50 Cremophor EL/ethanol to mimic the clinical formulation of paclitaxel (i.e., Taxol®), PTX-eNPs manufactured using the historical, in situ polymerization method, or PTX-eNPs manufactured using the pilot-scale, LV1 method. The saline and Taxol-mimic treatments had median survivals of 39 and 55 days, respectively, which agrees with previously published survival data in this model [10]. The historical PTX-eNPs and pilot-scale PTX-eNPs both significantly improved survival compared to these controls and never even reached a median survival metric due to survival of $>$60% of both groups until the end of the study at 90 days (Fig. 10E). Survival was not was not significantly different between the two PTX-eNP formulations indicating that the changes implemented as part of the pilot-scale method of production did not alter the in vivo efficacy of the PTX-eNPs.

3. Conclusion

Pilot-scale production of nanoparticles is an essential step in the process of clinical translation and commercialization. Our previously developed sonication-based miniemulsion and in situ polymerization manufacturing method is not scalable. However, using a new process that leverages commercially available Microfluidizer technology, we achieve pilot-scale production while maintaining the target particle diameter and PDI, as well as swelling functionality and in vivo safety and efficacy. The small diameter and low PDI of these

LV1-produced particles also enable sterilization via filtration—an important consideration in the clinical translation of this technology due to its low cost and ease of use. Future directions will include the further optimization of the current processes and attempts to remove particularly hazardous, toxic or costly materials, such as halogenated solvents. Through sharing these results, as well as our pitfalls and alternative strategies, with the broader research community, others may learn from this work and accelerate the translation of their own nanoparticle-based technologies.

4. Methods

4.1. Synthesis of eNP monomer precursor

Molecular sieves were activated via oven heating the day prior to use and stored in a round bottom flask overnight under vacuum while cooling. 500 g of 2,4,6-trimethoxybenzaldehyde, 459 g of 1,1,1-tris (hydroxymethyl)ethane and 20 L of tetrahydrofuran were charged to the reactor at 25 ± 5 °C and the reaction mass stirred under nitrogen for 50 min until all solids were dissolved. 1 kg of 3 Å molecular sieves were charged to the reactor at 25 ± 5 °C and the reaction mass stirred under nitrogen for 30 min. p-toluene sulfonic acid (PTSA) monohydrate was charged to a covered 1 L round bottom flask with 500 mL of THF and mixed until all solids were dissolved. This mixture was rapidly charged to the reactor through a funnel and the reaction solution mixed for 16 h at 180 rpm under nitrogen atmosphere. 50 g of sodium carbonate was charged to the reaction mixture and stirred for 30 min. The reaction mixture was removed by the bottom drain valve and filtered through a 1 mm metal sieve mesh to remove the sieves. The filtered solution was concentrated via roto-evaporation at 30 °C until all solvents were removed. In a separate container, 7 L of deionized purified water and 2 L of saturated sodium carbonate solution were charged and stirred until homogenous. ½ of this aqueous sodium carbonate mixture was charged to the concentrated reaction solid followed by ~10 L of methylene chloride. The mixture was homogenized and transferred back to the reactor where it was stirred at 200 rpm for 15 min. The agitation was stopped and the solution allowed to fully separate before draining the organic layer and keeping any rag layer with the aqueous fraction. This washing procedure was repeated with the other ½ of the aqueous sodium carbonate mixture. All organic phases were combined and dried over 1 kg of sodium sulfate, then filtered to remove solids. The solution was concentrated via roto-evaporation at 30 °C to give white/yellow solids which were dried at room temperature overnight under vacuum. The reaction yield was 98%.

4.2. Synthesis of eNP monomer

1000 g of the eNP monomer precursor and 30 L of DCM were charged to a 50 L reactor at 25 ± 5 °C under nitrogen and agitated 30 min until all solids were dissolved. 770 g of trimethylamine was charged to the 50 L reactor and stirred for 30 min until all solids were dissolved. The jacket temperature was set to 0 °C and agitation continued. When the reaction solution reached 0 ± 5 °C, 630 g methacryloyl chloride dissolved in 1 L methylene chloride was slowly charged to the reactor over the course of at least 1.5 h. The reaction was mixed for 30 min before being allowed to warm to room temperature overnight while mixing. In a separate container, 3 L of deionized purified water and 3 L of saturated sodium carbonate

solution were charged and stirred until homogenous. ½ of this aqueous sodium carbonate mixture was slowly charged to the reactor and stirred at 200 rpm for 30 min. The agitation was stopped and the solution allowed to fully separate before draining the organic layer and keeping any rag layer with the aqueous fraction. This washing procedure was repeated with the other ½ of the aqueous sodium carbonate mixture. All organic phases were combined and dried over 1 kg of sodium sulfate, then filtered to remove solids. The solution was concentrated via roto-evaporation at 30 °C to give white/yellow solids in a viscous orange liquid which were collected on a Buchner filter funnel and washed with acetate/heptane. Any orange-colored solids were recrystallized from 60 °C methanol and all solids were dried at room temperature overnight under vacuum. The reaction yield was 84%.

4.3. High performance liquid chromatography (HPLC) analysis of eNP monomer purity

The eNP monomer was evaluated for purity on a Varian Prostar HPLC system with UV-detector and Hamilton reverse phase C18 HxSil (5 um) column (Part No. 79869). The eluent was 70: 30, acetonitrile: water with a flow rate of 0.5 mL/min and detection at 254 nm.

4.4. Synthesis of PTX-eNPs using “historical”, in situ polymerization and probe-sonicator emulsification

eNP monomer (25 mg/mL) and paclitaxel (1.25 mg/mL, 0.05 wt/wt equiv.) were dissolved in 2.5 mL of dichloromethane and sodium dodecyl sulfate (12 mg/mL, 0.24 wt/wt equiv.) dissolved in 10 mM pH 7.4 phosphate buffer (10 mL). The aqueous and organic phases were sonicated under argon atmosphere for 30 min (1 s pulse with 2 s delay at 20% amplitude) in an ice bath using a Misonix probe-sonicator while stirring the solution with a stir-bar. Following emulsification, tetramethylethylenediamine (10 uL) and 200 mM ammonium persulfate (100 uL) were added to the reaction and this was allowed to stir for 4 h under argon and overnight under air. Particles were then dialyzed against 5 mM pH 7.4 phosphate buffer (1 L) and the buffer exchanged one time over 24 h.

4.5. HPLC analysis of PTX loading

Paclitaxel loading of the PTX-eNPs was measured by HPLC. A 50 uL aliquot of PTX-eNPs was diluted in 950 uL of acetonitrile with 0.1% trifluoroacetic acid (TFA). The dilution was vortexed for 60 s and filtered with a 0.22 um syringe tip filter prior to analysis via HPLC. HPLC detection of PTX was performed using a 20 min linear gradient from 60:40 to 35:65 water/acetonitrile +0.1% TFA at a flow rate of 0.5 mL/min on a Hamilton PRP-C18 5 um 250 × 2 column and Varian ProStar HPLC with detection at 254 nm.

4.6. Polymerization of eNP monomer

1300 g of the eNP monomer and 6.5 L of anisole (methoxybenzene) were charged to a 10 L reactor at 25 ± 5 °C under nitrogen and agitated for 30 min until all solids were dissolved. 2.91 g of AIBN was then also charged to reactor and mixed until all solids were dissolved. Subsurface sparge was performed for 1 h while agitating the solution after which the subsurface probe was removed and the reaction heated to an internal temperature of 70 °C while mixing under nitrogen for 16 h. The solution was allowed to cool to room temperature and 1.5 L of methylene chloride was added and stirred for 30 min. 33 L of

methanol was charged to a 50 L reactor and the solution agitated. The reaction was charged from the 10 L reactor to the 50 L reactor slowly over 1 h and then stirred for 30 min at 100 rpm. All solids were collected by vacuum filtration and suction dried for 5 min then collected and returned to the 50 L reactor for further washing. The methanol wash was repeated with fresh methanol and solids collected and dried again. The solids were rinsed with 5 L of fresh methanol on a Buchner funnel and collected and dried in a vacuum at 40 ± 5 °C. A white solid product was obtained in 80% yield.

Smaller scale (10 g) reactions were run with varying concentrations of AIBN to evaluate the impact of AIBN on eNP polymer MW prior to the above pilot-scale synthesis.

4.7. Characterization of eNP polymer molecular weight

The eNP polymer molecular weight was determined via gel permeation chromatography (GPC). The instrument setup consisted of a Wyatt Technology Interferometric Refractometer Detector (model: OPTILAB DSP), Rainin Instrument Co. Inc. HPXL Solvent Delivery System, Rainin Pressure Module and Waters Styragel® HR 5E DMF Column (Part No. WAT044229). Dilutions of eNP polymer were made at 2 mg/mL in running buffer (DMF with 0.05 M LiBr) and samples calibrated with and EasiCal PS1-B (polystyrene) standard (Agilent Technologies, Part No. PL2010–0501). With a flow rate of 0.5 mL/min the eNP polymer presents as a single peak from ~15–22 min.

4.8. Synthesis of PTX-eNPs using LV1 Microfluidizer

eNP polymer (25 mg/mL) and paclitaxel (1.25 mg/mL, 0.05 wt/wt equiv.) were dissolved in 50 mL of dichloromethane and sodium dodecyl sulfate (12–48 mg/mL, 0.24–0.96 wt/wt equiv.) dissolved in 10 mM pH 7.4 phosphate buffer (200 mL). The aqueous and organic phases were sonicated under argon atmosphere for 30 min (1 s pulse with 2 s delay at 20% amplitude) in an ice bath using a Misonix probe-sonicator while stirring the solution with a stir-bar. The emulsion was then processed on the LV1 Microfluidizer at 15,000 PSI (100 mPa) using an F12Y reaction chamber cooled in an ice bath. After processing 250 mL of nanoparticles through three passes, these were set aside and stirred under air for 4 h to allow the dichloromethane to evaporate (quantified by headspace analysis). Additional 250 mL batches of particles were synthesized to generate 1 L. Particles were then dialyzed against 5 mM pH 7.4 phosphate buffer (4 L per batch) and the buffer exchanged once over 24 h.

Smaller scale (20 mL) production runs were used to evaluate the impact of surfactant concentration and number of LV1 processing passes on eNP diameter and PDI. Particle diameter and PDI were measured using a Brookhaven DLS. Samples were diluted 100× in deionized water prior to measurement.

4.9. Dialysis tubing, sterile filtration and lyoprotection impact on PTX-eNPs

A single batch of 40 mL of PTX-eNPs was synthesized and divided into four equal volumes. The four volumes were dialyzed using either 10 kDa, 50 kDa, 300 kDa or 1000 kDa molecular weight cut off (MWCO) dialysis using the standard buffers and volume ratios described above. The buffers were exchanged once over 24 h at which point solution

volumes were measured and particles characterized by DLS. This study was repeated three times.

Sterile filtration was performed by manufacturing a 25 mL batch of PTX-eNPs and filtering the solution using a 0.22 um polyethersulfone (PES) syringe-tip filter. Significant back pressure is not evolved during filtration. Size and PDI were evaluated by DLS and PTX loading by HPLC, as above. This study was repeated three times.

PTX-eNPs were lyophilized by flash freezing them in liquid nitrogen followed by immediate transfer to a VirTis lyophilizer maintained at −39.5 °C and < 100 mTor for 48 h. Various lyoprotectants (glucose, sucrose, lactose, maltose, trehalose, mannitol) were evaluated by dissolving them into the PTX-eNP solution at 1%, 2%, 5% or 10% wt/vol at room temperature prior to filtration and freezing/lyophilization. Lyophilized particles were resuspended in the deionized water at the same concentration as pre-lyophilization and gently swirled for 2 min to ensure complete dissolution. Particle diameter was characterized by DLS.

Long term stability of lyoprotected, filtered, lyophilized PTX-eNPs was evaluated by storing particles in vials sealed with rubber stoppers and one-time-use metal crimp caps. Samples were maintained at 25 °C + 60% RH or 40 °C + 75% RH in closed ovens with humidity content maintained through the use of evaporative salt baths.

4.10. eNP swelling via SEM

Nanoparticles were diluted 1000× into 10 mM pH 7.4 phosphate buffer or 10 mM pH 5.0 acetate buffer and allowed to swell for 24 h. A 10 uL sample of each was then dried on a silicon wafer and the sampled sputter coated with a ~ 5 nm Au/PD layer prior to imaging (Cressington 108 Manual Sputter Coater; Zeiss Supra 40VP Field Emission Scanning Electron Microscope).

4.11. In vivo tumor model

Tumor model studies were performed at Massachusetts General Hospital, Boston, MA. Six- to eight-week-old, female, athymic, nude (NU/J) mice from Jackson Laboratory were housed under specific-pathogen-free conditions. Animal care and procedures were conducted with institutional Animal Care and Use Committee approval, in strict compliance with all federal and institutional guidelines for the care and use of laboratory animals. Mice received an intraperitoneal injection of 5×10^6 MSTO-211H-luc cells yielding established tumors followed by random assignment into treatment groups 7 days after tumor xenografting.

4.12. PTX-Rho-eNP tumor localization in vivo

Three weeks after xenografting, animals received an intraperitoneal injection of PTX-Rho-eNPs (10 mg PTX/kg body weight). At 24 h following PTX-Rho-eNP injection, animals were sacrificed and high-resolution digital photographs were taken of the intraperitoneal space using a Canon PowerShot A640 camera under ambient and ultraviolet (254 nm) light from a Wood's lamp.

4.13. PTX-eNP in vivo toxicity

Toxicity studies were performed at Augusta University, Augusta, GA using eight-week-old, female C57BL/6 mice from Jackson Laboratory. Animal care and procedures were conducted with institutional Animal Care and Use Committee approval (Protocol #2008–0162), in strict compliance with all federal and institutional guidelines for the care and use of laboratory animals. Animals ($N = 3$/group) received an intraperitoneal injection of PTX-eNPs (10 mg PTX/kg body weight) or saline. Body weight was measured daily for 14 days. Fourteen days later, animals were sacrificed, blood taken for analysis and liver and kidney harvested and processed for hematoxylin and eosin (H&E) staining and histopathological evaluation.

4.14. Comparison of pilot-scale and “historical” PTX-eNP efficacy in vivo

One week following xenografting, animals ($N = 8$/group) received the first of four weekly doses, administered intraperitoneally, of: pilot-scale PTX-eNPs, “historical” PTX-eNPs, paclitaxel dissolved in 50/50 Cremophor EL/ethanol (Taxol® mimic), or saline. All PTX treatments were given at 10 mg/kg/wk. (~250 μg PTX/injection) totaling ~1 mg over four weeks. Long-term survival was assessed with daily follow-up and individual sacrifice upon evidence of morbid disease progression.

4.15. Statistics

Data are presented as mean ± standard deviation unless specified in the text. Overall survivals were described by the Kaplan-Meier method and compared via log-rank test. All computations were done in SAS v9.2 for Unix or Prism 9.0 software. All significance tests and quoted P-values are two-sided with $P < 0.05$ being significant.

Supplementary Material

Refer to Web version on PubMed Central for supplementary material.

Acknowledgement

The authors acknowledge funding support from the NIH Small Business Innovation Research (SBIR) Program, including: R43 CA189215, R43 CA213538, and R44 CA189215. The authors would also like to acknowledge additional funding sources, including: R01 CA227433, R01 CA232056, R43 CA250780 and the Thoracic Surgery Foundation (NQC). Lastly, the authors would like to thank Christopher Jones, Bauer LeSavage and Nicholas Hall for their work in piloting the LV1 studies.

References

[1]. FDA, Guidance for Industry Considering Whether an FDA-Regulated Product Involves the Application of Nanotechnology. Services, U. S, 2014.

[2]. FDA, Drug Products, Including Biological Products, that Contain Nanomaterials Guidance for Industry. Services, U. S. D. o. H. a. H., Ed, 2017.

[3]. FDA, FDA’s Approach to Regulation of Nanotechnology Products. https://www.fda.gov/scienceresearch/specialtopics/nanotechnology/ucm301114.htm.

[4]. Langer K, Balthasar S, Vogel V, Dinauer N, von Briesen H, Schubert D, Optimization of the preparation process for human serum albumin (HSA) nanoparticles, Int. J. Pharm. 257 (1–2) (2003) 169–180. [PubMed: 12711172]

[5]. Karnik R, Gu F, Basto P, Cannizzaro C, Dean L, Kyei-Manu W, Langer R, Farokhzad OC, Microfluidic platform for controlled synthesis of polymeric nanoparticles, Nano Lett. 8 (9) (2008) 2906–2912. [PubMed: 18656990]

[6]. Singh D, McMillan JM, Kabanov AV, Sokolsky-Papkov M, Gendelman HE, Bench-to-bedside translation of magnetic nanoparticles, Nanomedicine (London, England)9 (4) (2014) 501–516.

[7]. Merkel TJ, Herlihy KP, Nunes J, Orgel RM, Rolland JP, DeSimone JM, Scalable, shape-specific, top-down fabrication methods for the synthesis of engineered colloidal particles, Langmuir26 (16) (2010) 13086–13096. [PubMed: 20000620]

[8]. Colby AH, Berry S, Paison K, Liu R, Colson YL, Ruiz-Opazo N, Grinstaff MW, Herrera V, Highly specific and sensitive fluorescent Nanoprobes for image-guided resection of sub-millimeter peritoneal tumors, ACS Nano11 (2) (2017) 1466–1477. [PubMed: 28099801]

[9]. Colby AH, Oberlies NH, Pearce CJ, Herrera VL, Colson YL, Grinstaff MW, Nanoparticle drug-delivery systems for peritoneal cancers: a case study of the design, characterization and development of the expansile nanoparticle, Wiley Interdiscip. Rev. Nanomed. Nanobiotechnol. 9 (3) (2017).

[10]. Liu R, Colby AH, Gilmore D, Schulz M, Zeng J, Padera RF, Shirihai O, Grinstaff MW, Colson YL, Nanoparticle tumor localization, disruption of autophagosomal trafficking, and prolonged drug delivery improve survival in peritoneal mesothelioma, Biomaterials102 (2016) 175–186. [PubMed: 27343465]

[11]. Griset AP, Walpole J, Liu R, Gaffey A, Colson YL, Grinstaff MW, Expansile nanoparticles: synthesis, characterization, and *in vivo* efficacy of an acid-responsive polymeric drug delivery system, J. Am. Chem. Soc. 131 (2009) 2469–2471. [PubMed: 19182897]

[12]. Colby AH, Colson YL, Grinstaff MW, Microscopy and tunable resistive pulse sensing characterization of the swelling of pH-responsive, polymeric expansile nanoparticles, Nanoscale5 (8) (2013) 3496–3504. [PubMed: 23487041]

[13]. Stolzoff M, Ekladious I, Colby AH, Colson YL, Porter TM, Grinstaff MW, Synthesis and characterization of hybrid polymer/lipid Expansile nanoparticles: imparting surface functionality for targeting and stability, Biomacromolecules16 (7) (2015) 1958–1966. [PubMed: 26053219]

[14]. Herrera VL, Colby AH, Tan GA, Moran AM, O'Brien MJ, Colson YL, Ruiz-Opazo N, Grinstaff MW, Evaluation of expansile nanoparticle tumor localization and efficacy in a cancer stem cell-derived model of pancreatic peritoneal carcinomatosis, Nanomedicine (London)11 (9) (2016) 1001–1015.

[15]. Abdelwahed W, Degobert G, Stainmesse S, Fessi H, Freeze-drying of nanoparticles: formulation, process and storage considerations, Adv. Drug Deliv. Rev. 58 (15) (2006) 1688–1713. [PubMed: 17118485]

[16]. Chen G, Wang W, Role of freeze drying in nanotechnology, Dry. Technol. 25 (1) (2007) 29–35.

[17]. Fonte P, Soares S, Sousa F, Costa A, Seabra V, Reis S, Sarmento B, Stability study perspective of the effect of freeze-drying using Cryoprotectants on the structure of insulin loaded into PLGA nanoparticles, Biomacromolecules15 (10) (2014) 3753–3765. [PubMed: 25180545]

[18]. Colson YL, Liu R, Southard EB, Schulz MD, Wade JE, Griset AP, Zubris KA, Padera RF, Grinstaff MW, The performance of expansile nanoparticles in a murine model of peritoneal carcinomatosis, Biomaterials32 (2011) 832–840. [PubMed: 21044799]

[19]. Colby AH, Liu R, Schulz MD, Padera RF, Colson YL, Grinstaff MW, Two-step delivery: exploiting the partition coefficient concept to increase Intratumoral paclitaxel concentrations in vivo using responsive nanoparticles, Sci. Rep. 6 (2016) 18720. [PubMed: 26740245]

[20]. Chu NQ, Liu R, Colby A, de Forcrand C, Padera RF, Grinstaff MW, Colson YL, Paclitaxel-loaded expansile nanoparticles improve survival following cytoreductive surgery in pleural mesothelioma xenografts, J. Thorac. Cardiovasc. Surg. 160 (3) (2020) e159–e168. [PubMed: 32044093]

[21]. Gilmore MD, Schulz MM, Liu MR, Zubris PKAV, Padera MRF, Catalano SPJ, Grinstaff PMW, Colson MYL, et al., Ann. Surg. Oncol. 20 (5) (2013) 1684–1693. [PubMed: 23128939]

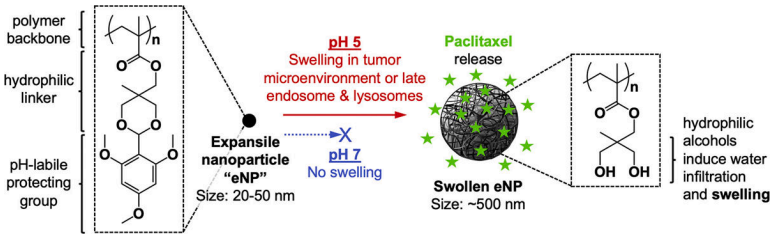

Fig. 1.

Schematic of expansile nanoparticle (eNP) structure and pH-responsive swelling functionality.

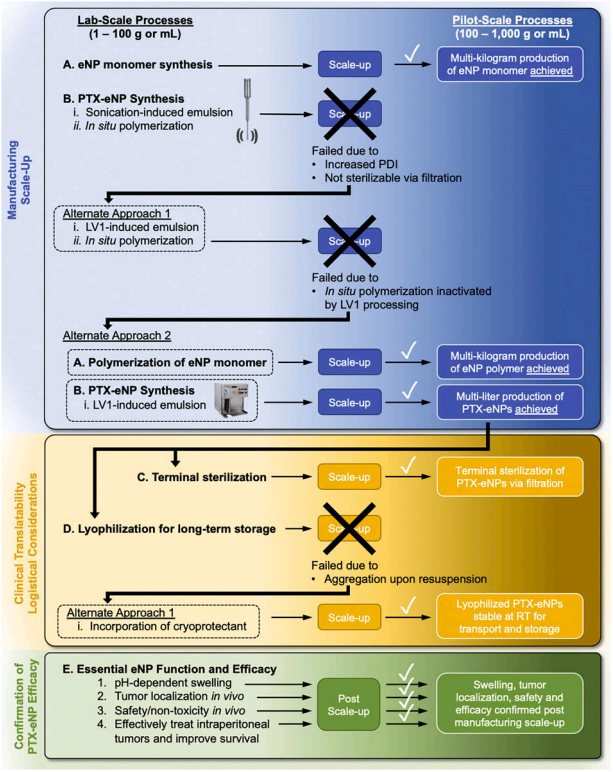

Fig. 2.

Summary of the scale-up process, including: successes, failures and alternative approaches.

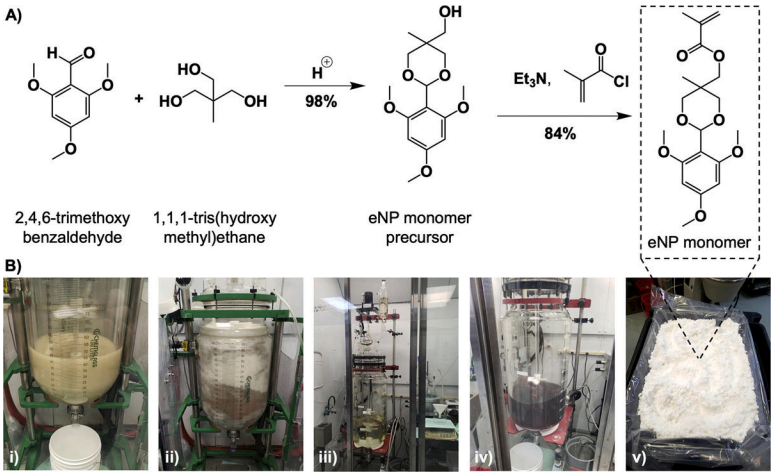

Fig. 3.

A) Synthetic schematic of the two-step route to the eNP monomer starting from commercially available materials. B) Photographs of eNP monomer precursor formation before (i) and after (ii) reaction completion as well as eNP monomer reaction before (iii) and after (iv) completion; v) ~1 kg eNP monomer.

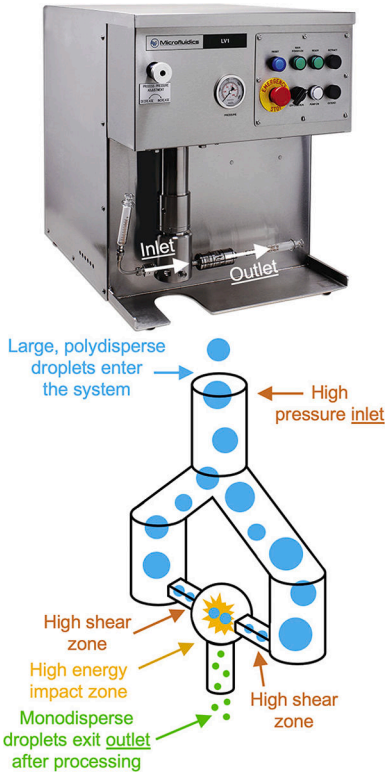

Fig. 4.

LV1 Microfluidizer schematic of operation. Polydisperse emulsions are injected into the system and driven at high pressure through microfluidic channels. The high-energy collisions lead to high shear forces on the droplets, reducing droplet size. Increased homogeneity in droplet sizes is obtained by processing the entire solution through the same high-shear conditions.

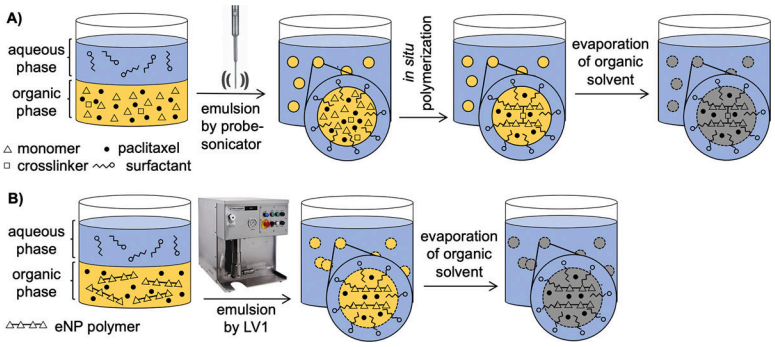

Fig. 5.

Schematic demonstrating the A)"historical" synthetic route via a probe sonicator-induced emulsion with in situ polymerization compared to the B) new, pilot-scale method employing an LV1-induced mini-emulsion of eNP polymer.

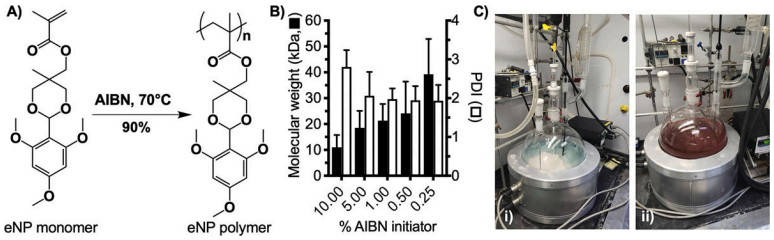

Fig. 6.

Synthesis and characterization of the eNP polymer. A) Schematic of the eNP polymerization reaction. B) The MW and PDI of the eNP polymer are dependent upon the amount of AIBN initiator. C) Photographs of polymerization before (i) and after (ii) reaction completion.

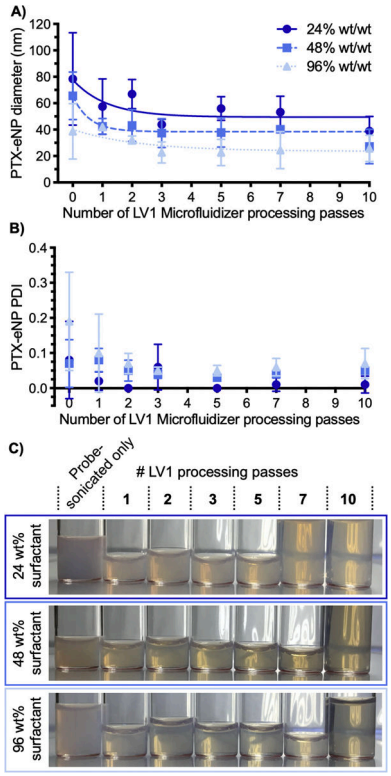

Fig. 7.

A) Impact of surfactant and LV1 processing on eNP diameter and PDI as measured via dynamic light scattering (DLS). With increasing weight % (wt%) of surfactant, particle diameter (A) and PDI (B) decrease. Processing with the LV1 up to three passes continually reduces eNP diameter and PDI; additional processing has no significant effect. C) Visual assessment of eNPs of differing surfactant incorporations and processing passes. After 2–3 LV1 passes, the solutions become more translucent, indicating a smaller and more uniform particle size distribution which corroborates the DLS results.

Fig. 8.
Photograph of 1 L of paclitaxel-loaded eNPs manufactured using the LV1 demonstrating the feasibility of pilot-scale production.

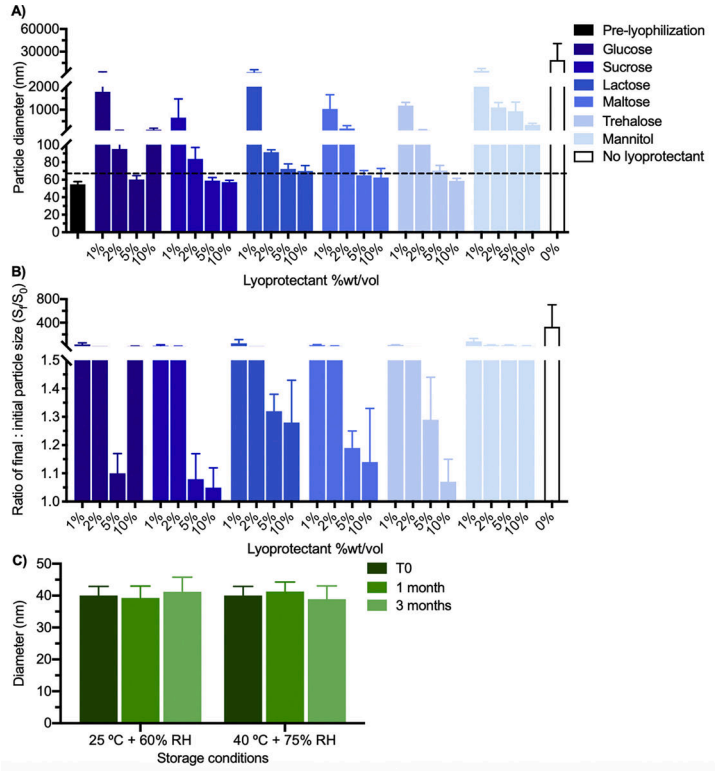

Fig. 9.

A) eNP diameter as a function of lyoprotectant composition and concentration. B) Ratio of post-lyophilization diameter to pre-lyophilization diameter (S_f/S_0) as a function of lyoprotectant composition and concentration. C) eNP diameter over 3 months at ambient and accelerated storage conditions.

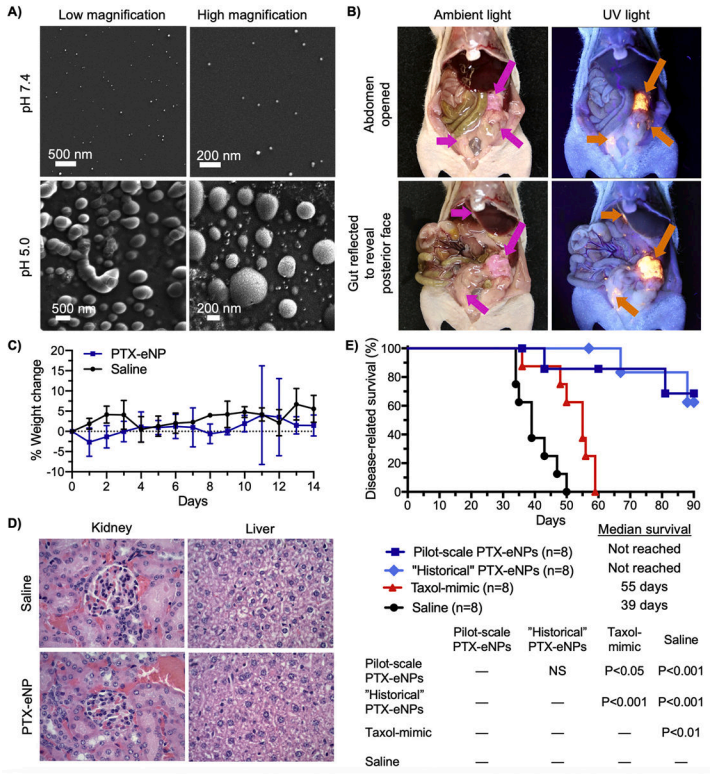

Fig. 10.

A) Expansile nanoparticles synthesized via LV1 processing are exposed to pH 7.4 (top row) or pH 5 (bottom row). After 24 h, eNPs at pH 7.4 have not changed in diameter (~40 nm) whereas particles exposed to pH 5 have swollen 2- to 10-fold. B) Paclitaxel-loaded rhodamine-labeled eNPs (PTX-Rho-eNPs) administered intraperitoneally to animals bearing establish mesothelioma xenografts localize specifically to tumors. Tumors (pink arrows) are visible under ambient light (left column) while PTX-Rho-eNP (orange arrows) are visible under UV light (right column). C) Healthy mice receiving intraperitoneal injections of PTX-eNPs (10 mg PTX/kg body weight) demonstrate no gross toxicity or difference in body weight compared to saline-injected controls. D) H&E staining of kidney and liver from these same animals demonstrates no observable difference between PTX-eNP and saline groups. E) Mice bearing established intraperitoneal mesothelioma tumors received four weekly treatment injections and were monitored for survival.”Historical” in situ polymerized PTX-eNP and pilot-scale, LV1 processed PTX-eNP both demonstrate significant improvements in survival compared to the clinical formulation (i.e., Taxol®)-mimic and saline control while exhibiting no statistical difference from each other. (For interpretation of the references to colour in this figure legend, the reader is referred to the web version of this article.)